2024 آب العدد 14
No.14 Aug 2024
المجلة العراقية للبحوث الإنسانية والإجتماعية والعلمية
Iraqi Journal of Humanitarian, Social and Scientific Research
Print ISSN 2710-0952 Electronic ISSN 2790-1254

Simulink Models of Monocrystalline and Polycrystilline silicon solar modules Considering Atmospheric Ambient Conditions

Tbarak Thamer Fadil
Emad Talib Hashim
Department of Energy Engineering, College of Engineering, University of Baghdad, Baghdad, Iraq
t.fadhil1709@coeng.uobaghdad.edu.iq[1], emadt@uobaghdad.edu.iq[2]

Abstract

The new study examines the effects of temperature fluctuations (25 ºC and 50 ºC) and changing solar radiation levels (500 and 1000 W/m²) on the output current, voltage, and power of monocrystalline and polycrystalline solar modules. A model with four parameters:I_{ph},I_o,R_s, and A.was utilized to develop simulation software for researching and evaluating the effects of temperature, wind, and solar radiation on solar panel output power. A one-diode model is used to develop an enhanced Simulink model that takes wind speed, solar module temperature, and irradiance into account all at once. Relative errors and root mean square error are also assessed to help prioritize the new work over an alternate strategy. The four parameter model's fitness is correlated with lower average root mean square error (RMSE) values. The computed RMSE was the difference between the estimated current-voltage values from the four-parameter model and the observed values. Under 1000 W/m^2 of solar radiation and 25°C solar module operating temperature, the root mean square error between the observed and predicted voltage-current characteristic is found to be at its lowest value of 0.025 for monocrystalline and for poly crystalline0.034

Keywords: Silicon, Solar Energy.

نمارج Simulink لوحدات الطاقة الشمسية أحادية البلورية والسيليكون متعدد البلورات مع مراعاة الظروف الجوية المحيطة

تبارك ثامر فاضل
عماد طالب هاشم
قسم هندسة الطاقة، كلية الهندسة، جامعة بغداد، بغداد، العراقالخلاصة

تبحث الدراسة الجديدة في آثار تقلبات درجات الحرارة 25 درجة مئوية و50 درجة مئوية وتغير مستويات الإشعاع الشمسي 500 و1000 واط/م2 على تيار الخرج والجهد والطاقة للوحدات الشمسية أحادية البلورية ومتعددة البلورات. نموذج ذو أربع متغيرات: التيار الضوئي(Iph) ، التشبع الداكن (Io)، مقاومة السلسلة (Rs) وعامل مثالية الدايود .(A) تم إستخدامه لتطوير برمجيات محاكاة لبحث وتقييم تأثيرات درجة الحرارة والرياح والإشعاع الشمسي. على طاقة انتاج الألواح الشمسية. يتم استخدام نموذج أحادي الصمام لتطوير نموذج Simulink المحسّن الذي يأخذ سرعة الرياح ودرجة حرارة الوحدة الشمسية والإشعاع في الاعتبار في وقت واحد. يتم أيضًا تقييم الأخطاء النسبية وجذر متوسط مربع الخطأ للمساعدة في تحديد أولويات العمل الجديد على استراتيجية بديلة. ترتبط ملاءمة نموذج المعلمات الأربعة بقيم أقل لمتوسط جذر متوسط مربع الخطأ .(RMSE) كان RMSE المحسوب هو الفرق بين قيم الجهد الحالي المقدرة من نموذج المعلمات الأربعة والقيم المرصودة. تحت 1000 واط/م2 من الإشعاع الشمسي ودرجة حرارة تشغيل الوحدة الشمسية البالغة 25 درجة مئوية، وجد أن

2024 آب العدد 14 المجلة العراقية للبحوث الإنسانية والإجتماعية والعلمية
No.14 Aug 2024 Iraqi Journal of Humanitarian, Social and Scientific Research
Print ISSN 2710-0952 Electronic ISSN 2790-1254

جذر متوسط مربع الخطأ بين خاصية تيار الجهد المرصودة والمتوقعة هو عند أدنى قيمة له وهي 0.025 للأحادي البلورية وللبلورات المتعددة 0.034 .). ويظهر أيضًا أن أقل نسبة خطأ للطاقة هي 0.6% وأعلى نسبة خطأ هي 5.7%. تم تحقيق أعلى نسبة أخطاء لوحدة الطاقة الشمسية متعددة البلورات أكثر من 24%
كلمات مفتاحية : سليكون ، طاقة شمسية

1.Introduction

Nowadays, approximately 80% of the energy that is delivered comes from polluting, depleting energy sources like fossil energy sources. The atmosphere is harmed through the emissions that are Presently produced through the burning of fossil energy sources, leading to major and irreversible environmental issues such acid rainfall, the The destruction of the ozone layer and greenhouse gas emissions (**Dincar,2003**). Because solar energy is fuel-free, sustainable, and kind to the environment, it ranks among the most important clean energy sources sources. As a result, research into PV systems and its uses isconstantly growing. Photovoltaic devices are electrical energygenerating semiconductor buildings from solar radiation. Solar power plants, application electrical automobiles and water pumping, satellite systems, and communication systems are just a few of the numerous uses for PV systems. The two main factors of photovoltaic energy outputs are cell temperature and radiationPresently, 90% of the Traditional monocrystalline and polycrystalline silicon cells with diffused junction make up the majority of options for photovoltaic panels.(**Pizzin,S.2012**), (**Rein,S.,2006**.), (**Tiwari,2009**), One of the main components of a photovoltaic system is photovoltaic panell, which directly turns sun's rays to electricity (**Ebrahimi, et al., 2019**). (**Catelani, et al., 2016**). The rendition of the PV(photovoltaic) modules is typically assessed Given typical test circumstances (STC). The sun spectrum averaged at AM 1.5 is employed, along with 1000 W/m2

Natural radiation and a maximum panel temperature of 25^{o}C (**Cattin, et al., 2019**).The impact of temperature in the electric yield bounds of the solar-powered module was investigated in a preliminary manner, and their temperature coefficients, which are crucial for planning and estimating in all systems, were determined.. (**Hashim, et al., and Akram et al., 2016**). Single-diode, double-diode, and empirical models are the three primary models used for solar cells and modules. Because of its simplicity and small number of factors, the empirical model is the most widely employed. Despite the two-diode model's accuracy, its complexity prevents it from being employed. Because it takes into account every parameter required to accurately represent a photovoltaic system, the one-diode model is more appropriate. Shunt resistance, series resistance, ideality factor, and reversed saturated current are the four main parameters. The values of these parameters vary depending on the models that came before them. (**Wang, et al., 2011**), (**Ramos-Hernanz, et al., 2012**)(**Aly, and El-Aal, 2005**), (**González-Longatt, 2005**), (**Altas, and Sharaf, 2007**),(**Sera, et al., 2007**), (**Houssamo, et al., 2010**), (**El Tayyan,**

2011(. In order to find the energy collected from solar PV collectors and to evaluate the solar PV performance parameters in Iraq, experimental simulations were conducted.,) **AlNajjar, 2013**(,)**Al-Najjar, 2015**(.and choosing the wrong points may lead to significant inaccuracy in the parameters being calculated and more work is being done to track the maximum power point and model solar panels. (**Hashim et al., 2018; Sarah et al., 2019)**. **Zainab and Ade**l(**Almukhtar and Merabet 2016**). The work's objective is to assess how weather conditions affect two types of solar photovoltaic modules: monocrystalline and polycrystalline, each of which is dependent on cell temperature, wind speed, and radiation as indicated by the characteristic curve IV. further to retrieve the solar energy module's four parameters. The relevant measured data and the model's output are contrasted. n order to confirm and verify the outputs of the simulation model. The suggested work has been finished in order to determine the ideal values for solar module parameter extraction. I_{ph} is photocurrent, R_s is series resistance, and I_0 is dark saturation current, A is diode ideality.

2.Experimental Setup:

In this work, a monocrystalline and polycrystalline silicon solar modules is used. To get more accurate statistics and comprehend the basic behavior of the panel, it is essential to experiment with photovoltaic panels in real-world settings. The experimental measurements took place over the course of six months, from July 2023 to January 2024. Using the Prova 200 solar module analyzer attributes, a solar module scan was performed for 10 seconds with a variable load of 0-∞ W (see Figure 1 and Table1).The laptop will get the measured data (I, V, and P) from this device. Figure 2 shows the connecting cables that go to the solar module's terminal.

Table 1. summerized solar module analyzer (prova 200) proparities

Batterery type	Rechargeable,2500mAh(1.2V)*8
AC Adaptor	AC 110V or 220V input DC 12V/ 1~3A output
Dimension	257(L)*155(W)*57(H)mm
Weight	1160g
Operation environment	0ºC~50ºC ,85%RH (relative humidity)
Temperature coefficient	0.1% of full scale/ºC (<18ºC or >28ºC)
Storage environment	-20ºC ~60ºC,75%RH
accessories	User manual * 1, AC adaptor*1 Optical USP cable*1 Software CD*1,software

		manual*1 Kelvin clips(6A max)*1 set
DC voltage measurements		
Range	**Resolution**	**Accuracy**
0-6	0.001V	±1% ±(1%of V_{open} 9mV)
6-10V	0.001V	±1% ±(1%of V_{open} 0.09mV)
10-60V	0.01V	±1% ±(1%of V_{open} 0.09mV)
DC current measurements		
Range	**Resolution**	**Accuracy**
0.01-6A	0.1mA	±1% ±(1%of I_{short}
0.6-61A	0.1mA	1%(1% of I_{short} 0.9mA)
1-6A	1mA	1%(1% of I_{short} 0.9mA)

Table 2. Solar panel properties.

	mc-Si	Pc-Si
Area, m^2	0.26	0.46
V_{oc}, V	22	23
I_{sc}, A	1.9	1.7
V_m, V	17.00	17.45
I_m, A	1.760	1.375
P_m, W	30	26
Ns	36	40
TCO of open-circuit voltage, □ (μ_{Voc}) V/°C	-0.0734	-0.0912
TCO of short-circuit current, □ (μ_{Isc}) A/°C	0.0003	0.0044
TCO of max. power, □ (μ_{P_m}) W/°C	-0.1353	-0.915

المجلة العراقية للبحوث الإنسانية والإجتماعية والعلمية
Iraqi Journal of Humanitarian, Social and Scientific Research
Print ISSN 2710-0952 Electronic ISSN 2790-1254

Figure 1. solar module analyzer(prova200).

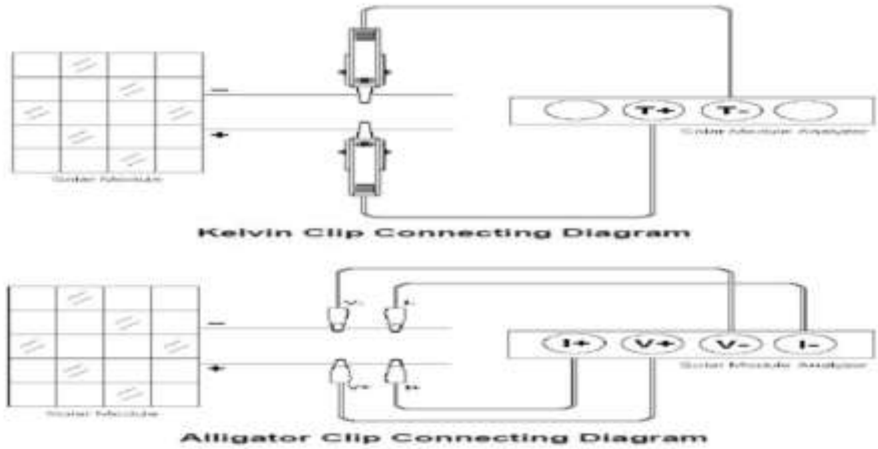

Figure 2. Wires connections.

3.Simulation block and modeling

(Bellini et al., 2009) served as the foundation to the model this paper proposes**.** The PV model's simplified equivalent circuit concept appears in Figure 3. The photovoltaic(PV)current is computed as a function of voltage in this model. Just the datasheet values for PV cell were used to run the model. In the proposed model, irradiance, solar cell temperature, and wind speed are the input parameters, and Photovoltaic current, Photovoltaic voltage, and Photovoltaic power are the output parameters. The Photovoltaic panel output current (I) is determined by the Photovoltaic output voltage (V). Photovoltaic modules are modeled using the following mathematical formula:

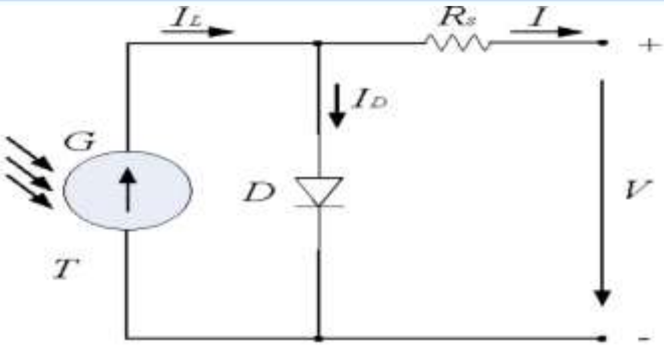

Figure 3. Simplified equivalent circuit model.

$$I = I_{sc}\left[1 - K_1\left(e^{(V/(K_2\, V_{oc}))} - 1\right)\right], \qquad (1)$$

Where

$$K_1 = \left(1 - \frac{I_{mp}}{I_{sc}}\right) e^{(-V_{mp}/(K_2\, V_{oc}))},$$

$$K_2 = \frac{(V_{mp}/V_{oc}) - 1}{ln\left(1 - \left(\frac{I_{mp}}{I_{sc}}\right)\right)}. \qquad (2)$$

The coefficient K_1 and K_2 alter based on the parameters of the solar module. The following represents how these characteristics vary depending on the panel temperature and/or radiation (**Bellini et al., 2009**):

$$I_{sc}(G, T_c) = I_{scs}\frac{G}{G_s}[1 + (T_c - T_s)],$$

$$I_{mp}(G, T_c) = I_{mps}\frac{G}{G_s}[1 + (T_c - T_s)],$$

$$V_{oc}(T_c) = V_{ocs} + (T_c - T_s),$$

$$V_{mp}(T_c) = V_{mps} + (T_c - T_s). \qquad (3)$$

Prameters The values provided in the manufacturer's datasheet for the standard test environments (G_S= 1000W/m^2 and T_S= 25 C) are those I_{scs}, I_{mps}, V_{ocs}, and V_{mps} .The radiation and temperature of photovoltaic panel are shown by G and Tc, respectively. The temperature coefficient for current α and for voltage β . correspondingl. In certain research published in the literature, the temperature of photovoltaic panel is taken to be the same as the surrounding air, yet this isn't always the case. The PV cell temperature is determined in this study as a device of the variations in radiation and the ambient temperature.

(Equation 4)

$$T_c = T\left(\frac{0.32}{8.91 + (2xv_{wind})}\right) x\, G \qquad (4)$$

Where, T_c is cell temperature with ambient condition, T is ambient temperature ,G is the radiance and v_{wind} is wind speed. Furthermore, wind speed affects Photovoltaic panel temperature as well, and this factor is separately considered when determining the Photovoltaic panel temperature for each module:

Figure 4 shows the Simulink block diagram for the suggested PV model.

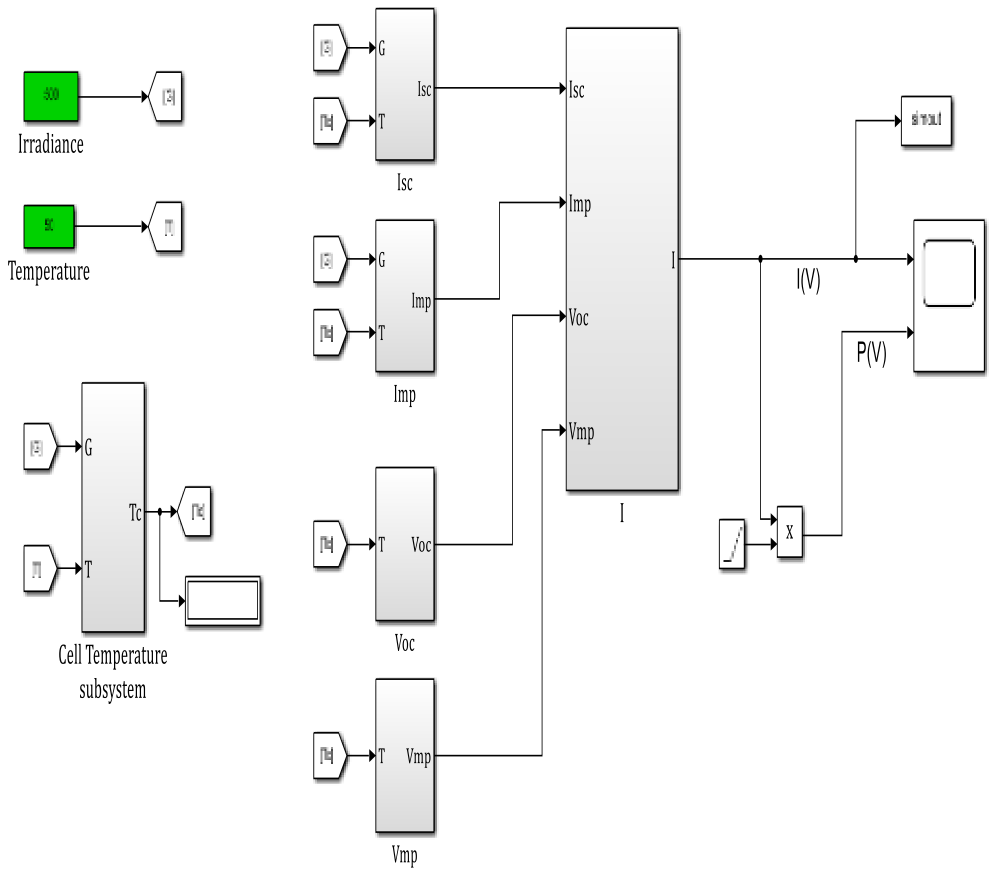

Figure 4. The Simulink block diagram related to proposed PV model.

Equation 4 calculates the panel's temperature while accounting for irredance, surrounding air temperature, and wind speed. It accomplishes this through using utilizing the solar module temperature block inside the Photovoltaic model's Simulink system. Photovoltaic cell voltage and current are measured using the load and evaluation block. Figure 3 displays the block diagram of photovoltaic cell subsystem. The solution to equations 1-3 yields the model shown in figure 5. The panel parameters block in the block schematic estimates the real values of these parameters from the temperature and irredance of the cell using the values of V_{oc}, I_{mp}, I_{sc}, and V_{mp} that were acquired under standard test conditions. Located in the block diagram is the Cell Current block situated in the block diagram, utilizes equation to acompute Photovoltaic current.

2024 آب العدد 14
No.14 Aug 2024
المجلة العراقية للبحوث الإنسانية والإجتماعية والعلمية
Iraqi Journal of Humanitarian, Social and Scientific Research
Print ISSN 2710-0952 Electronic ISSN 2790-1254

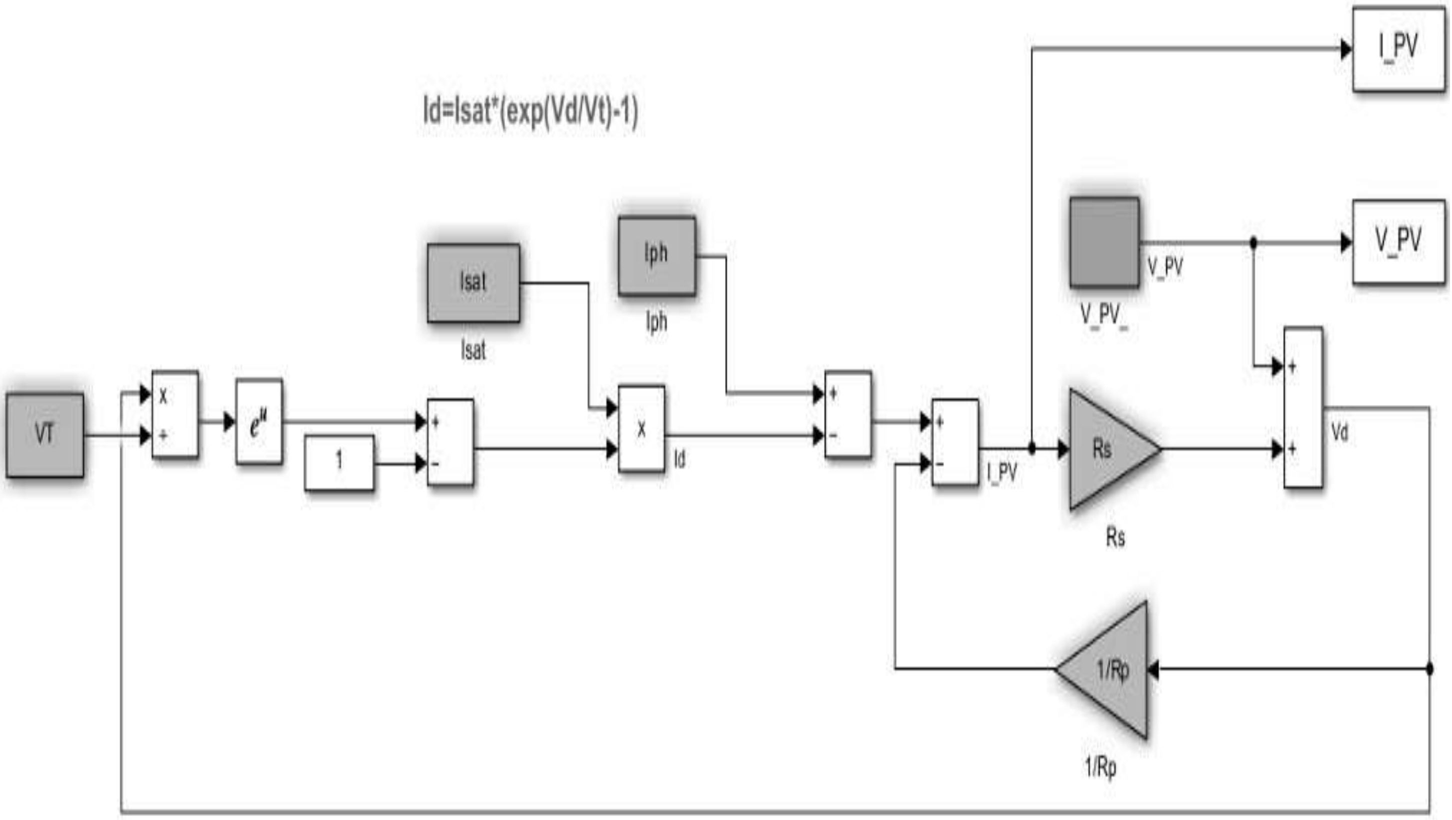

Figure 5. PV panel subsystem block diagram.

Matlab/Simulink models require temperature, wind speed, and radiance data recorded in real-world scenarios as input parameters. After that, using models, values for Photovoltaic power, voltage, and current were determined. The correctness of the model is verified by comparing the results of the simulation with the measured power levels of Photovoltaic cells in ambient settings. 16 figures are supplied for both monocrystalline and polycrystalline silicon panels, along with the relevant model outputs. Figures 6-9 will provide some examples.The graphic shows that the model's results primarily coincide with the findings of the experiment. The energy measurements derived from the model for the measuring time had only 3.1% for mono and 6.7% for poly divergence from the experimental values, according to a numerical evaluation

Figures,8,9 demonstrate the differences between the observed power outputs of polycrystalline silicon technology panels and the model output under various weather scenarios. As with monocrystalline technologies, the measured power values of polycrystalline silicon technology panel output do not exhibit a strong association with the data of the associated model (see Figures 6,7). Furthermore, a computational analysis revealed a 6.7% discrepancy between the energy value derived from the relevant model and the experimental findings. Based on this finding, it can be concluded that the proposed model is not very suitable for polycrystalline silicon panels.

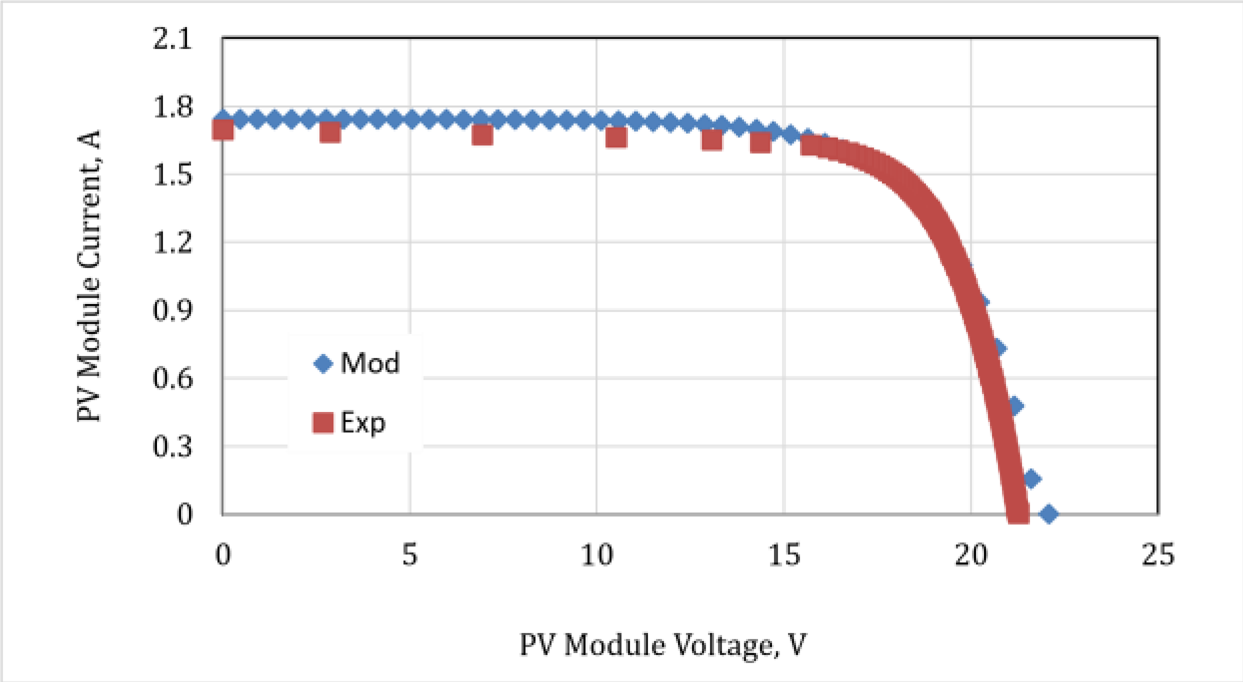

Figure 6. Current-voltage characteristic curve of monocrystilline solar module at solar radiation 1000 w/m^2 module temperature 25^{o}C.

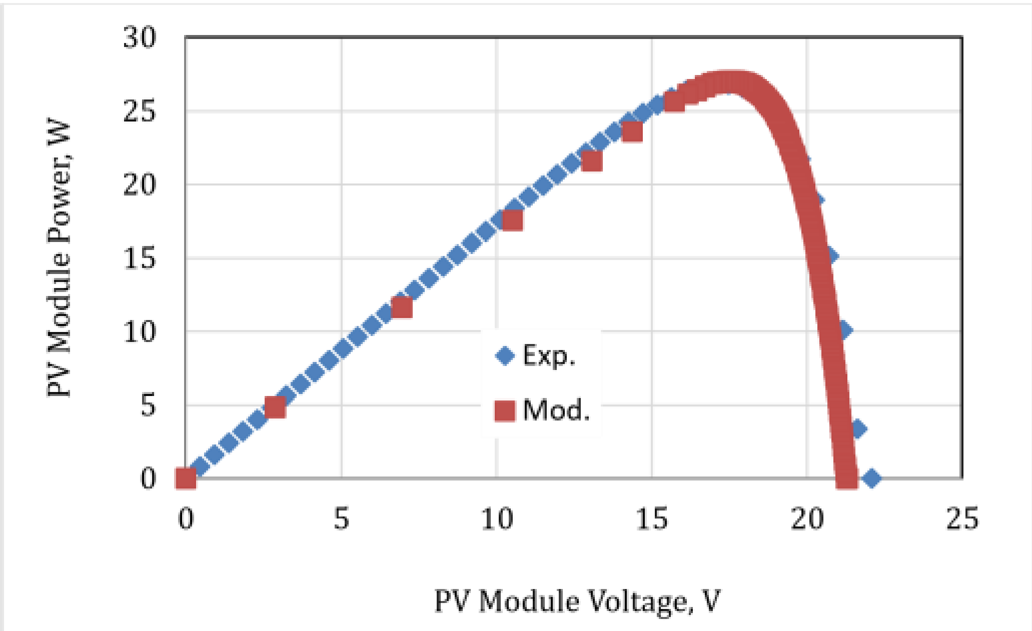

Figure 7. Power-voltage characteristic curve of monocrystilline solar module at solar radiation 1000 w/m^2 module temperature 25^{o}C.

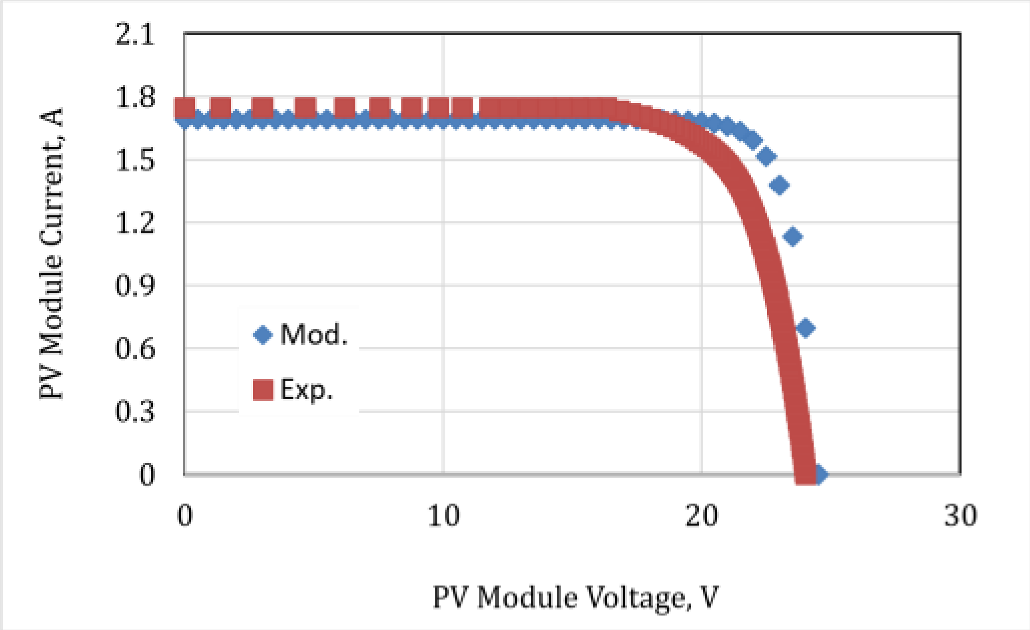

Figure 8. Current-voltage characteristic curve of polycrystilline solar module at solar radiation 1000 w/m^2 module temperature 25^{o}C.

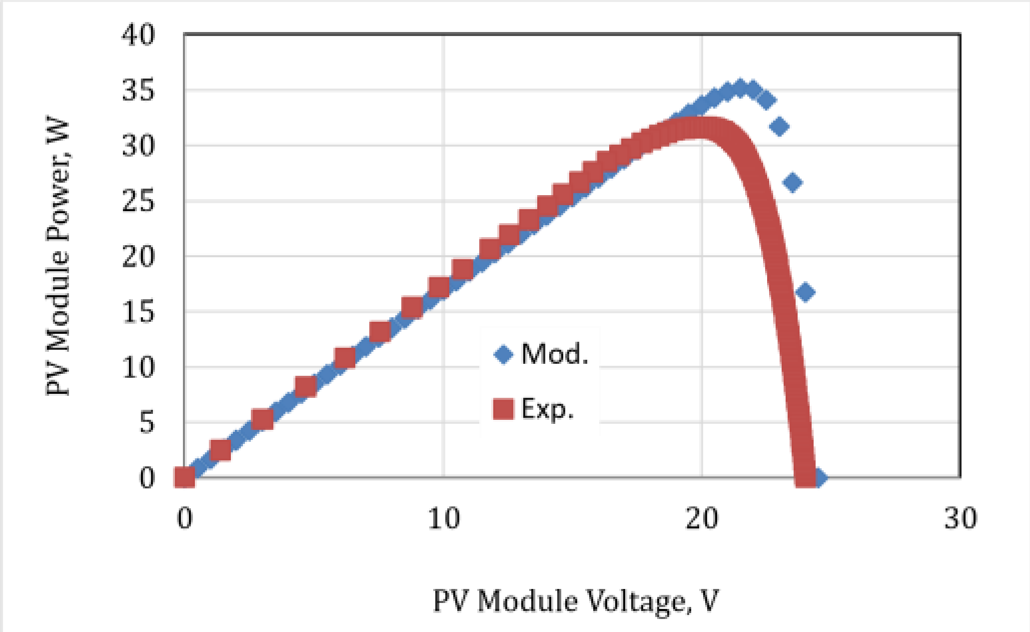

Figure 9. Power-voltage characteristic curve of polycrystilline solar module at solar radiation 1000 w/m^2 module temperature 25^{o}C.

4.Accuracy fitness of four-parameter model:

An excel sheet have the measured and calculated data at two radiation levels on six months, and to find out the fitness between the measured data and the corresponding modeled ones. Equation 5 gives the percentage of error between the measured values and calculated values (Matlab Simulink):

$$\frac{Laboratory\ measurments - Matlab\ Simulink}{Laboratory\ measurments} \times 100\% \qquad (5)$$

Table3 contains the measured operating solar module temperatures and solar module efficiencies at the two tested solar irradiance: 500 and 1000 Wm^{-2} and two solar module temperatures (25°C and 50°C). This table shows that the lowest percentage error for power is 0.6% and the highest one is 6.5%for monocrystalline and lowest percentage error for power is 0.9% and the highest one is 29.8%. The maximum power is attained at the highest solar radiation 1000 Wm^{-2} and the corresponding solar module temperature 25°C (at fixed solar irradiance, decreasing solar module temperature will be lead to increase efficiency and power output. That is due to decrease reverse saturation current).

Table 3. Comparisons of the measured values with the model results for monocrystilline and polycrystalline solar module at two solar irradiances; 500 and 1000 $w/m^2$and two solar model temperatures 25°C and 50°C

Solar radiation, Wm-2	Monocrystalline				Polycrystalline			
	500	**500**	**1000**	**1000**	**500**	**500**	**1000**	**1000**
TC, exp., oC	25	50	25	50	25	50	25	50
$P_{m,exp.}$, *W*	17.607	13.509	26.998	26.982	16.322	14.211	31.615	23.316
$P_{m,cal.}$, *W*	16.654	13.728	26.816	25.632	18.308	15.86	35.154	30.272
Error, %	5.7	-1.6	0.6	5.2	-12.2	-11.6	-11.2	-29.8
$I_{m,exp.}$, *A*	0.886	0.836	1.545	1.708	0.722	0.729	1.6	1.401
$I_{m,cal.}$, *A*	0.832	0.832	1.575	1.653	0.803	0.826	1.635	1.636
Error, %	6.5	0.4	-1.9	3.1	-11.2	-13.3	-2	-16.7
$V_{m,exp.}$, *V*	19.859	16.157	17.02	15.792	22.596	19.487	19.754	17.472
$V_{m,cal.}$, *V*	20.022	16.506	17.540	15.502	22.8	19.2	21.5	18.5
Error, %	-0.7	-2.1	-3.0	1.8	-0.9	1.4	-8.8	-5.8

Statistical work was done to calculate root mean square error (RMSE) (Ma et al., 1984):-

$$RMSE = \left(\frac{1}{n}\sum_{j=1}^{n}(I_{si}-I_{mi})^2\right)^{\frac{1}{2}} \quad (6)$$

Print ISSN 2710-0952 Electronic ISSN 2790-1254

Where n is the number of data, I_{si} is simulated current and I_{mi} is measured current.. The simulated model's correctness is satisfied and evaluated by the RMSE. Low RMSE values are correlated with increased formula (model) correctness. The estimated values of RMSE from the model are provided in Table 4. The fourparameter model's fitness was correlated with decreased RMSE average values. The root mean square error (RMSE) is 0.025 at 500 W/m2 of solar energy and 25°C solar module temperature. That is the mean near I-V calculated using I-V simulations.

Table 4. RMSE for the eight tested cases

	Test 1	Test 2	Test 3	Test 4
G, Wm^{-2}	500	500	1000	1000
Tc, °C	25	50	25	50
RMSE for monocrystalline	0.025	0.086	0.037	0.093
	Test 5	Test 6	Test 7	Test 8
G, Wm^{-2}	500	500	1000	1000
Tc, °C	25	50	25	50
RMSE for polycrystalline	0.035	0.034	0.071	0.075

Atmospheric temperature at which solar cells operate is decisively affected by temperature. Arise in solar module temperature causes a modest rise in short circuit current. However, open circuit voltage is extremely effect by increasing solar panel temperature more than 25°C.

Table 5. Measured and calculated V_{oc} and I_{sc} for the eight tested cases

Test No.	G, Wm-2	T_c, °C	V_{oc}, V			I_{sc}, A		
			measured	calculated	error, %	measured	calculated	error, %

1	500	25	23.978	25	-4.2	0.981	0.936	4.5
2	500	50	19.744	21	-6.3	0.928	0.954	-2.8
3	1000	25	21.284	22.08	-3.7	1.694	1.742	-2.8
4	1000	50	18.954	19.7	-3.9	1.941	1.919	1.1
5	500	25	26.971	25.8	4.3	0.867	0.841	2.9
6	500	50	23.792	22.2	6.7	0.898	0.852	5.1
7	1000	25	24.019	24.5	-2	1.743	1.69	3
8	1000	50	21.145	21.5	-1.6	1.779	1.712	3.7

Table 6. Maximum power drop comparisons with some previous work.

Study case	Present study	Hashim et al., 2016	Radziemska, 2003	Buday, 2011
%/ºC	0.46	0.45	0.65	0.5
Study case	El-Shaer et al., 2014	Spataru et al., 2014	Dash and Gupta 2015	
%/ºC	0.25	0.4546	0.446	

5. Conclusion

Taking into account the limitations of this investigation, the ensuing findings can be made from the research done: A universal Matlab/Simulink-created PV model that is typical of both PV cells and modules was tested using a monocrystalline and polycrystalline module. This model can be used as a tool for studying every type of PV module available on the market, especially how well they operate in different weather situations while following standard test procedures (STC). With solar irradiance, wind speed, and cell temperature as input factors and an output of the I-V and P-V characteristics under different conditions, the suggested model produces good results. For the tested modules, the Fill Factor appeared to be quite independent of temperature.It is therefore possible to ignore the impact of temperature on the parasitic internal resistances. Because of the high shunt resistance, there was no difference between the four and five parameter models for crystalline modules; the simplified four parameter model suffices.

Nomenclature

I: Photovoltaic output current

V: Photovoltaic output voltage

I_{SCS}: The standard test conditions (STC) for short circuit current

I_{MPS}: At STC, the maximum power point current

V_{OCS}: At STC, voltage of the open circuit

V_{MPS}: At STC Maximum power point voltage

I_{SC}: current short circuit

I_{MP}: Maximum power point current

V_{OC}: Open circuit voltage

V_{MP}: Maximum power point voltage

G: radiation

G_S: At STC (1000 W/m^2),radiation

T: Air temperature (∘C)

T_C: Temperature of the cell (∘C)

T_S: At STC (25^o C),Temperature

V_{wind}: Wind speed (m/s).

α: current temperature coefficient (A/^{o}C)

β: voltage temperature coefficient (V/^{o}C)

Reference:

1. Abdulameer A. Akram., “Temperature Effect on Power Drop of Different Photovoltaic Modules”, MSc. Thesis, Baghdad University, 2016.
2. Almukhtar, Zainab, and Adel Merabet. 2016. “Maximum Power Point Tracking Based on Estimated Power for PV Energy Conversion System.” 10(4):533–37.
3. Al-Najjar, H. M. T., 2013,Experimental Evaluation of the Performance of One-Axis Daily Tracking and Fixed PV Module in Baghdad, Iraq. Journal of Engineering 19(9): 1145-1157.

4. Al-Najjar, H. M. T.,2015,Study of Energy Gains by Orientation of Solar Collectors in Baghdad City. Journal of Engineering 21(10): 17-35.
5. Altas, I. and A. Sharaf .,2007, A Photovoltaic Array Simulation Model for Matlab-Simulink GUI Environment. Clean Electrical Power, 2007. ICCEP'07. International Conference on, IEEE.
6. Aly, A. E.-M. M. M., and A. El-Aal .,2005, Modeling and Simulation of a Photovoltaic Fuel Cell Hybrid System.
7. Bellini A., Bifaretti S., Iacovone V., Cornaro C.,2009. Simplified model of a photovoltaic module, Applied Electronics, IEEE (2009), pp. 47-5.
8. Catelani, M., Ciani, L., Kazimierczuk, M.K., and Reatti, A., 2016. Matlab PV solar concentrator performance prediction based on triple junction solar cell model. Measurement, 88, pp.310-317.
9. Cattin, J., Dupré, O., Aïssa, B., Haschke, J., Ballif, C., and Boccard, M., 2019. Optimized Design of Silicon Heterojunction Solar Cells for Field Operating Conditions. IEEE Journal of Photovoltaics, 9(6), pp.1541-1547.
10. Dincar, I., 2003, The Role of Energy in Energy Policy Making. Energy Policy Vol 30, PP. 137-149.
11. Ebrahimi, S.M., Salahshour, E., Malekzadeh, M., and Gordillo, F., 2019. Parameters identification of PV solar cells and modules using flexible particle swarm optimization algorithm. Energy, 179, pp.358-372.
12. El Tayyan, A. A. ,2011,PV system behavior based on datasheet. Journal of Electron Devices 9(20011): 335-341.
13. González-Longatt, F. M. ,2005,Model of Photovoltaic Module in Matlab. Ii Cibelec 2005: 1-5.
14. Hashim, E. T., and Talib, Z. R., 2018. Modeling and Simulation of Solar Module performance using Five Parameters Model by using Matlab in Baghdad City. Journal of Engineering, 24 (10),pp. 15-31.
    a. https://doi.org/10.31026/j.eng.2018.10.02
15. Houssamo, I., M. Sechilariu, F. Locment, and G. Friedrich., 2010,Identification of photovoltaic array Model parameters. Modeling and experimental verification. International Conference on Renewable Energies and Power Quality.
16. Li, Heng, Jun Peng, Weirong Liu, Zhiwu Huang, and Kuo Chi Lin. 2014. "A Newton-Based Extremum Seeking MPPT Method for Photovoltaic Systems with Stochastic Perturbations." International Journal of Photoenergy 2014. doi: 10.1155/2014/938526.
17. Ma, T, Yang, H. and Lu, L., 2014. Solar photovoltaic system modeling and performance prediction. Renew Sustain Energy Rev, 36, pp. 4–15. Doi: 10.1016/j.rser.2014.04.057.

18.Mohammed, M. S. , and Hashim, E. T., 2019. Characterization Performance of Monocrystalline Silicon Photovoltaic Module Using Experimentally Measured Data. Journal of Engineering , 25 (10), pp. 1-19.Doi.org/10.31026/j.eng.2019.10.01.

19.Pizzini, S. (Ed.). (2012). Advanced silicon materials for photovoltaic applications. John Wiley & Sons.

20.Ramos-Hernanz, J., J. Campayo, J. Larranaga, E. Zulueta, O. Barambones, J. Motrico, U. F.

21.Rein, S., 2006. Lifetime spectroscopy: a method of defect characterization in silicon for photovoltaic applications (Vol. 85). Springer Science & Business Media.

22.Tiwari, Gopal Nath, and Swapnil Dubey. Fundamentals of photovoltaic modules and their applications. Royal Society of Chemistry, 2009.

23.Sera, D., R. Teodorescu and P. Rodriguez ., 2007, PV Panel Model Based on Datasheet Values. Industrial Electronics, 2007. ISIE 2007. IEEE International Symposium on, IEEE.

24.Wang, J.-C., J.-C. Shieh, Y.-L. Su, K.-C. Kuo, Y.-W. Chang, Y.-T. Liang, J.-J. Chou, K.-C. Liao and J.-A. Jiang ., 2011, A Novel Method for the Determination of Dynamic Resistance for Photovoltaic Modules,Energy 36(10): 5968-5974.

المراجع

١. عبد الأمير أكرم، "تأثير درجة الحرارة على انخفاض الطاقة للوحدات الكهروضوئية المختلفة"، ماجستير. أطروحة، جامعة بغداد، 2016.

٢. المختار، زينب، وعادل مرابط. 2016. "تتبع الحد الأقصى لنقاط الطاقة بناءً على الطاقة المقدرة لنظام تحويل الطاقة الكهروضوئية." 10(4):533-37.

٣. النجار، H. M. T. 2013، التقييم التجريبي لأداء التتبع اليومي أحادي المحور والوحدة الكهروضوئية الثابتة في بغداد، العراق. مجلة الهندسة 19(9): 1145-1157.

٤. النجار، ح.م.ت،2015،دراسة مكاسب الطاقة بتوجيه مجمعات الطاقة الشمسية في مدينة بغداد. مجلة الهندسة 21(10): 17-35.

٥. ألتاس، آي. وأ. شرف.، 2007، نموذج محاكاة المصفوفة الكهروضوئية لبيئة واجهة المستخدم الرسومية Matlab-Simulink. الطاقة الكهربائية النظيفة، 2007. ICCEP'07. المؤتمر الدولي حول IEEE.

٦. علي، أ.م. م. م.، وأ. العال.، 2005، نمذجة ومحاكاة النظام الهجين لخلايا الوقود الكهروضوئية.

٧. بيليني أ.، بيفاريتي إس.، إياكوفون في.، كورنارو سي.، 2009. نموذج مبسط للوحدة الكهروضوئية، الإلكترونيات التطبيقية، IEEE (2009)، الصفحات 47-5.

٨. كاتي لان، M.، Ciani، L.، Kazimierczuk، M.K، and Reatti، A.، 2016. التنبؤ بأداء مكثف الطاقة الشمسية Matlab PV بناءً على نموذج الخلايا الشمسية ثلاثية الوصلات. القياس، 88، ص 310-317.

٩.كاتين، J., Dupré, O., Aïssa, B., Haschke, J., Ballif, C., and Boccard, M., 2019. التصميم الأمثل للخلايا الشمسية السيليكونية غير المتجانسة لظروف التشغيل الميدانية. مجلة IEEE

للخلايا الكهروضوئية، 9(6)، الصفحات من 1541 إلى 1547. ١٠. دينكار، آي، 2003، دور الطاقة في صنع سياسات الطاقة. سياسة الطاقة المجلد 30، ص. 137-149.

١١. إبراهيمي، إس إم، صلاحشور، إي، مالك زاده، إم، وجورديلو، إف، 2019. تحديد معلمات الخلايا والوحدات الشمسية الكهروضوئية باستخدام خوارزمية تحسين سرب الجسيمات المرنة. الطاقة، 179، ص 358-372.

١٢. أ. الطيان، 2011، سلوك النظام الكهروضوئي على أساس ورقة البيانات. مجلة الأجهزة الإلكترونية 9 (20011): 335-341.

١٣. غونزاليس لونجات، إف إم، 2005، نموذج الوحدة الكهروضوئية في ماتلاب. الثاني سيبيليك 2005: 1-5.

١٤. هاشم، ت.، وطالب، ز. ر.، 2018. نمذجة ومحاكاة أداء الوحدة الشمسية باستخدام نموذج خمسة معلمات باستخدام ماتلاب في مدينة بغداد. مجلة الهندسة، 24 (10)، ص. 15-31.
أ. https://doi.org/10.31026/j.eng.2018.10.02

١٥.حسامو، I., M. Sechilariu, F. Locment, and G. Friedrich., 2010، تحديد معلمات نموذج المصفوفة الكهروضوئية. النمذجة والتحقق التجريبي. المؤتمر الدولي للطاقات المتجددة وجودة الطاقة.

١٦. لي، هينغ، جون بينغ، ويرونغ ليو، زيوو هوانغ، وكو تشي لين. 2014. "البحث عن طريقة MPPT المستندة إلى نيوتن للأنظمة الكهروضوئية ذات الاضطرابات العشوائية." المجلة الدولية للطاقة الضوئية 2014. دوى: 10.1155/2014/938526.

١٧.ما، T, Yang, H. and Lu, L., 2014. نمذجة النظام الكهروضوئي الشمسي والتنبؤ بالأداء. Renew Sustain Energy Rev، 36، الصفحات من 4 إلى 15. دوى: 10.1016/j.rser.2014.04.057.

١٨. محمد، م.س.، وهاشم، إ.ت.، 2019. توصيف أداء الوحدة الكهروضوئية المصنوعة من السيليكون أحادي البلورية باستخدام البيانات المقاسة تجريبيًا. مجلة الهندسة، 25 (10)، ص 1- Doi.org/10.31026/j.eng.2019.10.01.19.

١٩. بيتزيني، س. (محرر). (2012). مواد السيليكون المتقدمة للتطبيقات الكهروضوئية. جون وايلي وأولاده.

٢٠. راموس هيرنانز، ج.، ج. كامبايو، ج. لاراناجا، إي. زولوتا، أو. بارامبونيس، ج. موتريكو، يو. إف.

٢١.رين، S., 2006. التحليل الطيفي مدى الحياة: طريقة لتوصيف العيوب في السيليكون للتطبيقات الكهروضوئية (المجلد 85). سبرينغر العلوم والإعلام التجاري.

٢٢. تيواري وجوبال ناث وسوابنيل دوبي. أساسيات الوحدات الكهروضوئية وتطبيقاتها. الجمعية الملكية للكيمياء، 2009.

٢٣.سيرا، D., R. Teodorescu and P. Rodriguez., 2007، نموذج اللوحة الكهروضوئية بناءً على قيم ورقة البيانات. الإلكترونيات الصناعية، 2007. ISIE 2007. ندوة IEEE الدولية حول IEEE.

٢٤. وانغ، جي.-سي، جي.-سي. شيه، Y.-L. سو، ك.-C. كو، Y.-W. تشانغ، Y.-T. ليانغ، J.-J تشو، K.-C. لياو وج.-أ. جيانغ، 2011، طريقة جديدة لتحديد المقاومة الديناميكية للوحدات الكهروضوئية، الطاقة 36(10): 5968-5974.